PLOS ONE

RESEARCH ARTICLE

# Construction of a high-density genetic map for grape using specific length amplified fragment (SLAF) sequencing

**Jiahui Wang☯, Kai Su☯, Yinshan Guo*, Huiyang Xing, Yuhui Zhao, Zhendong Liu, Kun Li, Xiuwu Guo***

College of Horticulture, Shenyang Agricultural University, Shenyang, Liaoning, P.R. China

☯ These authors contributed equally to this work.
* guoyinshan77@126.com (YSG); guoxw1959@163.com (XWG)





**Citation:** Wang J, Su K, Guo Y, Xing H, Zhao Y, Liu Z, et al. (2017) Construction of a high-density genetic map for grape using specific length amplified fragment (SLAF) sequencing. PLoS ONE 12(7): e0181728. https://doi.org/10.1371/journal.pone.0181728

**Editor:** Jean-Marc Lacape, CIRAD, FRANCE

**Received:** March 9, 2017

**Accepted:** July 6, 2017

**Published:** July 26, 2017



**Data Availability Statement:** All relevant data are within the paper and its Supporting Information files.

**Funding:** This work was supported by the National Natural Science Foundation of China (Grant No. 31372021, 31572085), and the China Agriculture Research System (CRAS-30-yz-6).

**Competing interests:** The authors have declared that no competing interests exist.

## Abstract

Genetic maps are important tools in plant genomics and breeding. We report a large-scale discovery of single nucleotide polymorphisms (SNPs) using the specific length amplified fragment sequencing (SLAF-seq) technique for the construction of high-density genetic maps for two elite wine grape cultivars, 'Chardonnay' and 'Beibinghong', and their 130 $F_1$ plants. A total of 372.53 M paired-end reads were obtained after preprocessing. The average sequencing depth was 33.81 for 'Chardonnay' (the female parent), 48.20 for 'Beibinghong' (the male parent), and 12.66 for the $F_1$ offspring. We detected 202,349 high-quality SLAFs of which 144,972 were polymorphic; 10,042 SNPs were used to construct a genetic map that spanned 1,969.95 cM, with an average genetic distance of 0.23 cM between adjacent markers. This genetic map contains the largest molecular marker number of the grape maps so far reported. We thus demonstrate that SLAF-seq is a promising strategy for the construction of high-density genetic maps; the map that we report here is a good potential resource for QTL mapping of genes linked to major economic and agronomic traits, map-based cloning, and marker-assisted selection of grape.

## Introduction

Grape (*Vitis vinifera* L., $2n = 38$) is one of the most important perennial fruit vines worldwide, with a production of 74 million tons over a harvested area of 7 million ha in 2014 (FAO, http://faostat3.fao.org/browse/Q/QC/E). The consumption of table grapes and/or wine has proven to be greatly beneficial to human health [1–4], and the demand for high-quality grapes has increased considerably in recent years. However, grape growth, yield, and quality are affected by various biotic and abiotic stresses. Therefore, for grape breeders, it is important to identify methods for improving the quality characteristics and stress resistance of cultivated grapes. This optimization can be achieved by crossing different germplasms from domesticated or wild-type grapes that possess the desired superior traits [5]. However, the generation using conventional breeding methods of grape cultivars with the preferred traits requires

considerable time and can even take decades. Thus, alternative methods are necessary to facilitate the rapid incorporation of these desirable traits in cultivars for large-scale production.

One such method involves the use of genetic maps; these provide a basis for QTL mapping, identification of functional genes, and marker-assisted selection. Genetic linkage maps, particularly high-density genetic maps, are one of the most valuable tools for QTL mapping and high-throughput superior trait selection among various germplasms, including plants and animals. They thus constitute an important means to identify and cultivate resistant, economically viable cultivars, and the construction of such maps is therefore important for grape breeding. Over the past two decades, several unsaturated grape genetic maps have been constructed based on DNA markers, such as randomly amplified polymorphic DNA (RAPD) [6,7], amplified fragment length polymorphism (AFLP) [8], sequence related amplified polymorphism (SRAP) [9], and simple sequence repeat (SSR) [10–12]. However, the application of RAPD, AFLP, and SRAP markers has thus far been limited owing to their dominant inheritance and low transferability. On the contrary, SSR markers have advantages such as co-dominant inheritance, reproducibility, and locus specificity for genetic map construction. However, the number of these markers is generally limited and some of the markers have no sequence information. The development of next-generation sequencing (NGS) technologies and the availability of the full grape genome sequence [13] have facilitated considerable development of single nucleotide polymorphism (SNP) markers [14]. SNPs are the most abundant and stable type of genetic variations in genomes and therefore play an important role in genetic map construction [15,16]. Several efficient NGS-based methods have been used to identify SNPs, such as restriction site associated DNA sequencing (RAD-seq) [17], 2b-RAD [18], double digest RAD (ddRAD) [19], genotyping-by-sequencing (GBS) [20], and specific length amplified fragment sequencing (SLAF-seq) [21]. RAD genotyping is measured by randomly digesting genomic DNA with restriction enzymes; 2b-RAD and ddRAD are derived methods of RAD where 2b-RAD is based on the use of type IIB restriction enzymes and ddRAD is a double-digest technology with two restriction enzymes. Methylation sensitive restriction endonuclease ApeKI is used to digest the genomic DNA in GBS, and SLAF is measured by sequencing the paired-ends of the sequence-specific restriction fragment length. SLAF-seq represents a high-resolution strategy for large-scale *de novo* SNP discovery and genotyping, and this approach has been successfully used to construct high-density genetic maps for many plant and animal species [22–26]. SLAF-seq is a powerful high-throughput technique for rapid and efficient development of SNP markers for genetic map construction.

In the present study, we employed two grape cultivars, 'Chardonnay' and 'Beibinghong'. 'Chardonnay', which was used as the female parent, is a grape with thin, yellow-green skin, mainly used for brewing white wine and champagne, and lacking high disease and pest resistance. The male parent, the *V*. *amurensis*-derived 'Beibinghong' with thick, dark blue skin, was first bred in northeast China and used for ice red wine production [27]. Moreover, it has high cold tolerance and disease resistance and can overwinter without soil covering in Ji'an, Jilin, China. 'Chardonnay' and 'Beibinghong' thus exhibit significant differences in several traits, such as skin color and thickness, fruit aroma, and resistance to diseases, and meet the requirements for mapping populations for high-density genetic map construction.

In this study, SLAF-seq was used for rapid discovery of SNPs in $F_1$ populations derived from a cross between the two wine grape cultivars. Subsequently, a high-density genetic map of grape was constructed and its characteristics were analyzed in detail. This map is a good potential resource for genetic or QTL mapping of major economic and agronomic traits, map-based cloning, and marker-assisted selection of grape varieties.

## Materials and methods

### Plant material and DNA extraction

A grape hybrid population derived from a cross of 'Chardonnay' (*V*. *vinifera*) and 'Beibinghong' (*V*. *amurensis* × *V*. *vinifera*) was generated in May of 2014. The female parent of 'Beibinghong' was 'Zuoyouhong' which was derived from the cross between $F_1$ of 'Zuoshaner' (*V*. *amurensis*) × 'Muscat Rouge' (*V*. *vinifera*) and '74-1-326' (*V*. *amurensis*). The male parent of 'Beibinghong' was '86-24-53' which was derived from the cross between $F_1$ of '73040' (*V*. *amurensis*) × 'Ugni Blanc' (*V*. *vinifera*) and 'Shuangfeng' (*V*. *amurensis*). A total of 331 individuals were produced, of which 130 individuals and their parents were used as the mapping population. The seedlings of the progeny and the parents were planted in the experimental orchard of Shenyang Agriculture University in Shenyang, Liaoning Province, China.

Healthy young leaves were harvested from both parents and each individual $F_1$ plant. The samples were immediately stored in liquid nitrogen and transferred to a -80˚C freezer. Genomic DNA was extracted using the cetyltrimethylammonium bromide (CTAB) method [28]. DNA concentration was measured using a NanoDrop spectrophotometer (ND2000; Thermo Fisher Scientific, USA) and DNA quality was determined by electrophoresis on 0.8% agarose gels.

### SLAF library construction and high-throughput sequencing

We used an improved SLAF-seq strategy [29]. Two enzymes, *Rsa*I and *Hae*III (New England Biolabs, USA), were used to digest the genomic DNA of each sample after marker discovery and SLAF pilot experiments. A single nucleotide (A) overhang was added subsequently to the digested fragments, and duplex tag-labeled sequencing adapters (PAGE-purified, Life Technologies, USA) were ligated to the A-tailed fragments. Polymerase chain reaction (PCR) was performed using diluted restriction-ligation DNA samples, dNTP, Q5®High-Fidelity DNA Polymerase, and PCR primers. The PCR products were then purified and pooled, and pooled samples were separated by 2% agarose gel electrophoresis. Fragments ranging from 400 to 450 bp (with indexes and adaptors) in size were excised and purified using a QIAquick gel extraction kit (Qiagen, Hilden, Germany). Gel-purified products were then diluted, and pair-end sequencing (each end 125 bp) was performed on an Illumina HiSeq 2500 system (Illumina, Inc., San Diego, CA, USA) according to the manufacturer's recommendations.

### Sequence data grouping and genotyping

Marker identification and genotyping were performed using procedures described by Sun et al. [21]. Briefly, low-quality reads (quality score $< 30$) were filtered out and then raw reads were sorted to each progeny. Clean reads from the same sample were mapped onto the PN40024 grape genome sequence [30] using BWA (0.7.10-r789) software [31] with parameters set to Score (missed match) = 3, Score (opening gap) = 11, and Score (gap extension) = 4. Sequences mapped to the same position were defined as a single SLAF locus with the depth and integrity thresholds of 7 and 0.3, respectively. Only SLAFs with two to four alleles were identified as polymorphic SLAFs. Genome Analysis Toolkit (GATK) [32] and Sequence Alignment/Map tools (SAMtools) [33] were used to identify SNP loci after local realignment with GATK. Considering the data accuracy, the intersection of SNP calls made by the two tools was regarded as the candidate SNP dataset, and only biallelic SNPs were retained as the final SNP dataset. Polymorphic markers were classified into four segregation patterns (hk × hk, lm × ll, nn × np, and aa × bb). Based on the population type of $F_1$, three segregation patterns (excluding aa × bb) were selected for genetic map construction. Genotype scoring was then performed

using a Bayesian approach to further ensure the genotyping quality [21]. High-quality SNP markers for genetic mapping were filtered and those with the average sequence depths of >40-fold in the parents and with less than 5% missing data were retained. The chi-square test was then performed to examine the segregation distortion, and markers with significant segregation distortion ($P < 0.05$) were initially excluded from map construction and added later as accessory markers.

### Linkage map construction

SNP markers were partitioned primarily into linkage groups (LGs) based on their locations on the grape genome. Next, the modified logarithm of odds (MLOD) scores between markers was calculated to further confirm the robustness of markers for each LG. Markers with MLOD scores < 5 were filtered prior to ordering. A HighMap strategy was applied to order the SNP markers and correct genotyping errors within LGs [34]. Briefly, recombinant frequencies and LOD scores were calculated using a two-point analysis and these were applied to infer linkage phases. Then, enhanced Gibbs sampling, spatial sampling, and simulated annealing algorithms were combined to conduct an iterative process of marker ordering [35,36]. The mapping algorithm was repeated until all markers were mapped appropriately. The error correction strategy of SMOOTH was then applied based on the parental contribution of genotypes [37], and a k-nearest neighbor algorithm was applied to impute missing genotypes [38]. Skewed markers were then incorporated into this map using the multipoint maximum likelihood method. Map distances were estimated using the Kosambi mapping function [39]. The collinearity between the genetic and physical positions, the haplotype map, and the heat map were used to evaluate the quality of the constructed linkage map. The methods were conducted as described by Liu et al. [40].

## Results

### Analysis of SLAF-seq data and markers

A total of 372.53 M paired-end reads were generated for this grapevine population; of those 91.92% were high quality, which corresponds to a quality score of at least 30 (Q30). The average guanine-cytosine (GC) content was 40.03%. The reads number in female and male parents was 11,355,661 and 9,702,794, respectively. On average, 2,767,511 reads per individual were generated (Table 1). Of a total of 202,349 high-quality SLAFs, 179,508 were detected in the female parent and 177,451 in the male parent; the average sequence depth of each SLAF from the parents was 33.81-fold and 48.20-fold for the female and male parents, respectively. The analysis of the mapping population revealed that 149,910 SLAFs were generated, and the average depth of each SLAF was 12.66-fold for each offspring (Fig 1).

Of these high-quality SLAFs, 181,337 were mapped onto the grape genome sequence and 144,972 were polymorphic with a polymorphism rate of 71.64%. A total of 1,762,745 SNPs were obtained. The number of SLAFs and SNPs in each chromosome differed; the number of SLAFs ranged from 7,601 in chromosome 17 to 12,883 in chromosome 18, while the number of SNPs ranged from 73,727 in chromosome 17 to 119,963 in chromosome 18 (Table 2). Of

**Table 1. Summary of SLAF-seq data for grape.**

| Samples | Total reads | SLAFs number | Total depth | Average depth |
|---|---|---|---|---|
| Female | 11,355,661 | 179,508 | 6,069,279 | 33.81 |
| Male | 9,702,794 | 177,451 | 8,553,213 | 48.20 |
| Offspring | 2,767,511 | 149,910 | 1,906,168 | 12.66 |

https://doi.org/10.1371/journal.pone.0181728.t001

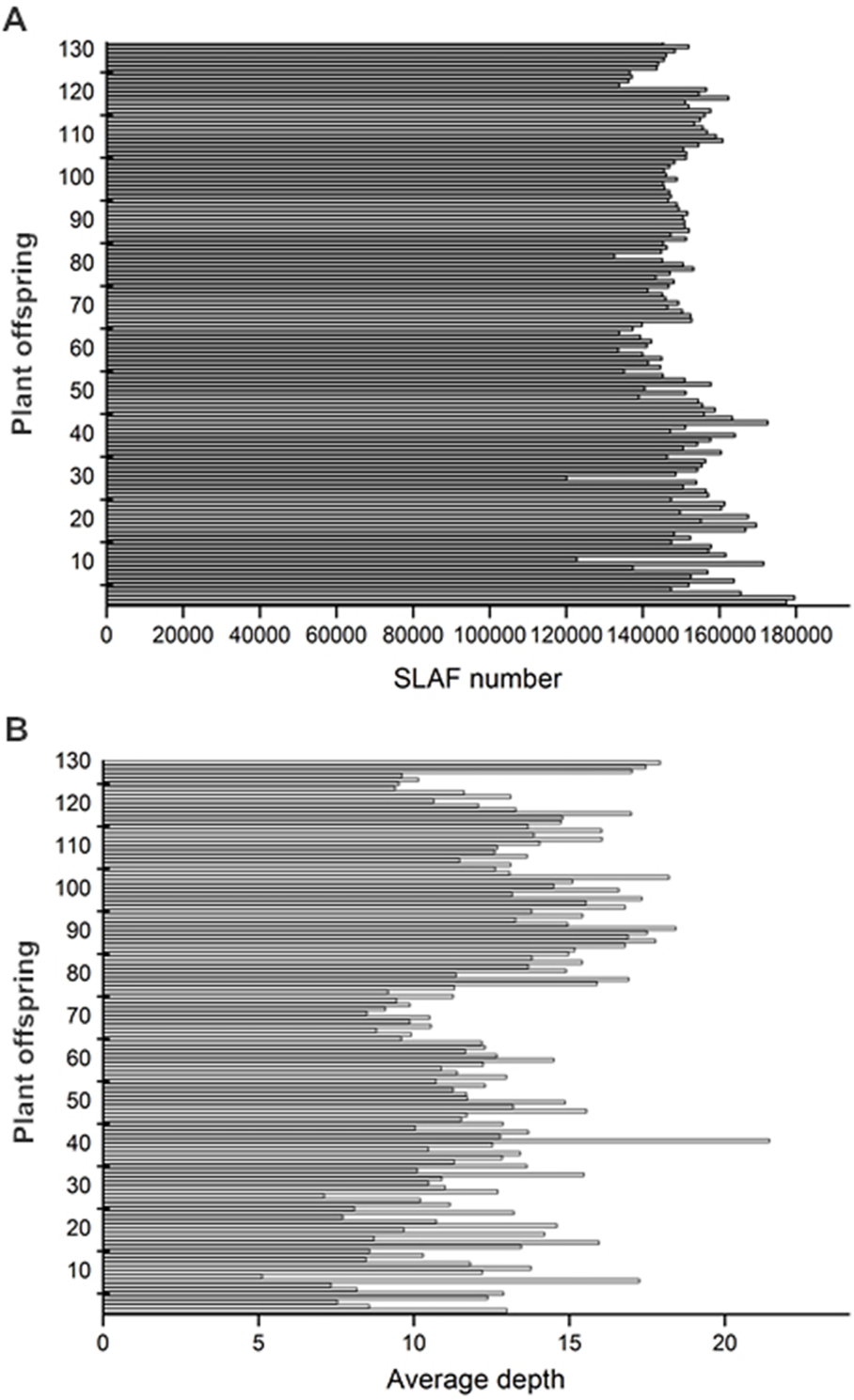


**Fig 1. Number of SLAFs (A) and average sequencing depths (B) of $F_1$ population.** The x-axis indicates the number of SLAFs (A) and the average depths (B); the y-axis indicates individual $F_1$ offspring.

https://doi.org/10.1371/journal.pone.0181728.g001

**Table 2. Distribution of SLAFs and SNPs on chromosomes.**

| Linkage groups ID | SLAFs number | SNPs number |
|---|---|---|
| LG1 | 10,019 | 93,391 |
| LG2 | 8,426 | 78,090 |
| LG3 | 8,815 | 79,777 |
| LG4 | 10,476 | 97,241 |
| LG5 | 11,315 | 107,752 |
| LG6 | 8,682 | 78,428 |
| LG7 | 8,503 | 78,629 |
| LG8 | 10,157 | 101,232 |
| LG9 | 8,438 | 92,920 |
| LG10 | 7,972 | 77,727 |
| LG11 | 8,853 | 80,038 |
| LG12 | 9,588 | 97,777 |
| LG13 | 10,591 | 100,828 |
| LG14 | 12,430 | 123,501 |
| LG15 | 8,808 | 91,325 |
| LG16 | 8,656 | 85,805 |
| LG17 | 7,601 | 73,727 |
| LG18 | 12,883 | 119,963 |
| LG19 | 9,724 | 104,594 |
| Total | 181,337 | 1,762,745 |

https://doi.org/10.1371/journal.pone.0181728.t002

the 1,762,745 polymorphic SNPs, 99,634 were biallelic and classified into four segregation patterns—aa × bb (22,460), hk × hk (7,240), lm × ll (40,618), and nn × np (29,316). Besides the aa × bb genotype, the other three patterns were used for genetic map construction, and a total of 77,174 SNPs fell into these classes (4.38% of total polymorphic SNPs).

## Characteristics of the genetic maps

All mapped markers fell into 19 LGs based on the chromosome numbers. There were 6,002 markers in the female map with a total length of 2,186.38 cM (Fig 2). The genetic length of each LG ranged from 86.18 cM (LG17) to 237.19 cM (LG18). LG14 contained the largest number of markers (518), with the average marker distance being 0.21 cM, whereas LG2 had the lowest marker number (163), with an average marker distance of 0.72 cM (Table 3). The percentage of 'Gap $\leq$ 5' (gaps wherein the distance between adjacent markers was smaller than 5 cM) for each LG ranged from 96.91% (LG2) to 99.81% (LG14) (Table 4).

The map of the male parent contained 4,740 markers spanning a total of 1,964.96 cM (Fig 3). LG4 was the shortest LG (length 74.05 cM) and contained 355 markers, with an average genetic distance of 0.21 cM, whereas LG6 was the longest group (length 119.15 cM) and contained 307 markers, with an average genetic distance of 0.39 cM (Table 3). The percentage of 'Gap $\leq$ 5' for each LG ranged from 79.49% (LG2) to 100.00% (LG3 and LG5) (Table 4).

The integrated grape map contained 10,042 markers spanning 1,969.95 cM with an average inter-marker distance of 0.23 cM (Fig 4). These 10,042 markers had an average coverage of 138.03-fold in the parents and 38.76-fold in the $F_1$ offspring. The genetic length of the LGs ranged from 77.21 cM (LG4) to 116.15 cM (LG18), with an average length of 103.68 cM. LG5 was the most saturated, spanning 104.02 cM with 872 markers and the average genetic distance of 0.12 cM, whereas LG2 was the least saturated with the length of 110.75 cM and contained the least number of markers (only 182) (Table 3). Moreover, the average percentage of 'Gap $\leq$ 5'

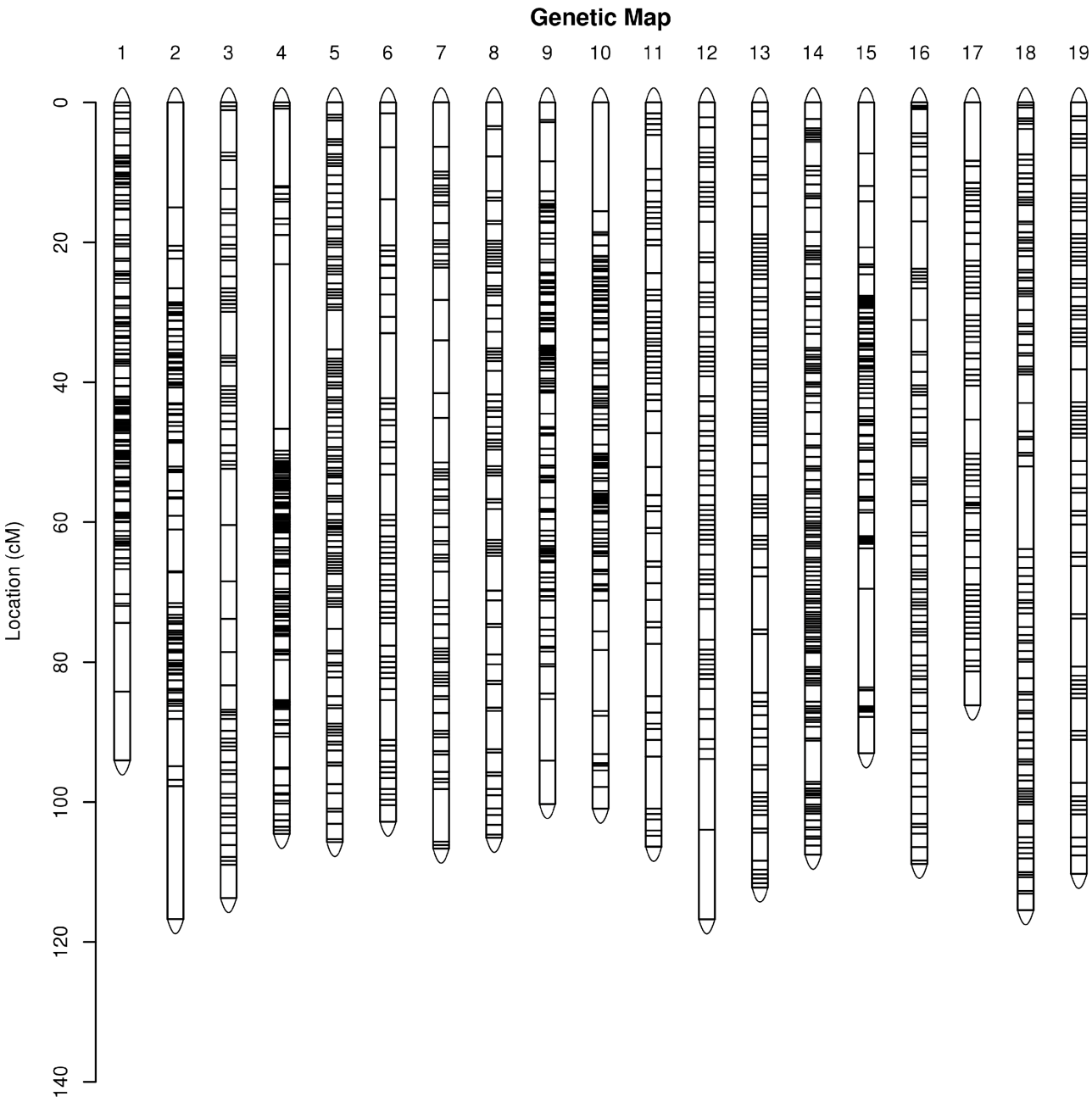


**Fig 2. Genetic map lengths and marker distribution in 19 linkage groups of the female parent.** Genetic distance is indicated by the vertical scale in centimorgans (cM). Black lines represent mapped markers. 1–19 represent corresponding linkage groups ID.

https://doi.org/10.1371/journal.pone.0181728.g002

was 99.69%. 'Gap $\leq$ 5' was not detected on LG4, LG5, LG6, LG7, LG13, LG14, LG18, and LG19 (Table 4); two gaps larger than 10 cM were located one in LG1 and one in LG2.

## Evaluation of the genetic map

The correlation of genetic and physical positions is an important factor in the quality of a genetic map [41]. The collinearity between the genomic location of mapped SNP markers and physical positions is presented in S1 Fig. The Spearman correlation coefficient in 19 LGs

**Table 3. The genetic length and markers number of 19 linkage groups.**

| Linkage groups ID | No of SNP markers | | | Genetic length (cM) | | | Physical length [a] (bp) |
|---|---|---|---|---|---|---|---|
| | Female map | Male map | Integrated map | Female map | Male map | Integrated map | |
| LG1 | 296 | 356 | 617 | 94.06 | 118.01 | 113.06 | 23037639 |
| LG2 | 163 | 40 | 182 | 116.74 | 116.13 | 110.75 | 18779844 |
| LG3 | 281 | 295 | 521 | 113.70 | 102.10 | 104.10 | 19341862 |
| LG4 | 322 | 355 | 581 | 104.56 | 74.05 | 77.21 | 23867706 |
| LG5 | 438 | 488 | 872 | 105.72 | 110.61 | 104.02 | 25021643 |
| LG6 | 274 | 307 | 530 | 102.81 | 119.15 | 116.06 | 21508407 |
| LG7 | 336 | 303 | 593 | 106.64 | 109.44 | 108.27 | 21026613 |
| LG8 | 342 | 217 | 556 | 105.11 | 105.76 | 105.94 | 22385789 |
| LG9 | 254 | 147 | 387 | 100.28 | 113.01 | 112.67 | 23006712 |
| LG10 | 230 | 156 | 349 | 100.95 | 92.17 | 101.83 | 18140952 |
| LG11 | 322 | 299 | 581 | 106.39 | 112.03 | 103.09 | 19818926 |
| LG12 | 375 | 267 | 611 | 116.76 | 107.14 | 115.87 | 22702307 |
| LG13 | 383 | 348 | 666 | 112.22 | 107.44 | 102.07 | 24396255 |
| LG14 | 518 | 241 | 747 | 107.55 | 102.52 | 103.55 | 30274277 |
| LG15 | 175 | 50 | 221 | 93.02 | 96.14 | 99.55 | 20304914 |
| LG16 | 191 | 196 | 347 | 108.84 | 75.38 | 71.42 | 22053297 |
| LG17 | 315 | 176 | 445 | 86.18 | 91.19 | 94.54 | 17126926 |
| LG18 | 432 | 320 | 711 | 237.19 | 107.57 | 116.15 | 29360087 |
| LG19 | 355 | 179 | 525 | 167.66 | 105.12 | 109.81 | 24021853 |
| Total | 6,002 | 4,740 | 10,042 | 2186.38 | 1964.96 | 1969.95 | 426176009 |

[a] Physical size is according to Jaillon et al. [30].

https://doi.org/10.1371/journal.pone.0181728.t003

ranged from 0.75 to 0.99, and it was higher than 0.92 in 73.68% of them (Table 5). The results indicated that the correlation of the genetic and physical positions was high in most LGs.

Haplotype and heat maps were also used to evaluate the quality of the genetic map. Haplotype maps can directly reflect recombination events in each individual. The occurrence of double crossovers and deletions is reflected in a haplotype map as genotyping and marker-order errors. Haplotype maps were generated for each $F_1$ individual and for the parental controls using 10,042 SNP markers as described by West et al. [42] (S1 File). There was no deletion detected in any LG.

Heat maps were also generated by using pair-wise recombination values for the 10,042 mapped SNP markers (S2 File). Additionally, heat maps can indicate the recombination between markers within one single LG; they could thus be used to identify potential marker ordering errors, pair-wise recombination taking place mainly as a result of hotspot regions for genomic recombination, and sequencing-related genotyping errors. In general, most LGs were determined to perform well.

## Discussion

### SLAF sequencing and large-scale marker development

The SLAF-seq strategy, a combination of locus-specific amplification and high-throughput sequencing, has been subjected to a series of critical trials to verify its high efficiency and accuracy of the generated markers [21]. Recently, the SLAF-seq technology has been used successfully to develop a large number of SLAF markers and for the construction of high-density

**Table 4. The markers spacing and coverage of 19 linkage groups.**

| Linkage groups ID | Average spacing (cM) | | | Gaps≤5 (Max Gap) | | | Coverage [b] (%) | | |
|---|---|---|---|---|---|---|---|---|---|
| | Female map | Male map | Integrated map | Female map | Male map | Integrated map | Female map | Male map | Integrated map |
| LG1 | 0.32 | 0.33 | 0.18 | 99.32% (9.84) | 98.59% (12.22) | 99.68% (11.81) | 99.04 | 99.72 | 99.72 |
| LG2 | 0.72 | 2.90 | 0.61 | 96.91% (19.00) | 79.49% (13.30) | 98.34% (10.52) | 92.51 | 94.12 | 94.12 |
| LG3 | 0.40 | 0.35 | 0.20 | 98.21% (8.04) | 100.00% (4.84) | 99.81% (5.02) | 99.16 | 99.58 | 99.58 |
| LG4 | 0.32 | 0.21 | 0.13 | 99.07% (23.52) | 99.72% (5.93) | 100.00% (4.50) | 99.84 | 99.43 | 99.84 |
| LG5 | 0.24 | 0.23 | 0.12 | 99.77% (5.60) | 100.00% (4.83) | 100.00% (2.36) | 99.84 | 99.70 | 99.84 |
| LG6 | 0.38 | 0.39 | 0.22 | 98.17% (9.27) | 99.35% (20.66) | 100.00% (4.84) | 99.47 | 98.70 | 99.47 |
| LG7 | 0.32 | 0.36 | 0.18 | 98.51% (7.55) | 98.34% (9.92) | 100.00% (4.96) | 99.68 | 99.92 | 99.92 |
| LG8 | 0.31 | 0.49 | 0.19 | 99.71% (5.49) | 98.61% (18.39) | 99.82% (5.42) | 99.68 | 99.50 | 99.68 |
| LG9 | 0.39 | 0.77 | 0.29 | 98.81% (8.80) | 96.58% (22.66) | 99.22% (9.78) | 99.79 | 98.43 | 99.79 |
| LG10 | 0.44 | 0.59 | 0.29 | 98.69% (15.53) | 98.71% (11.58) | 99.43% (9.57) | 99.29 | 98.79 | 99.29 |
| LG11 | 0.33 | 0.37 | 0.18 | 99.38% (7.45) | 97.99% (12.93) | 99.83% (6.71) | 99.89 | 99.89 | 99.89 |
| LG12 | 0.31 | 0.40 | 0.19 | 99.47% (12.81) | 98.50% (30.83) | 99.67% (6.40) | 99.33 | 98.36 | 99.33 |
| LG13 | 0.29 | 0.31 | 0.15 | 99.48% (8.39) | 99.14% (8.58) | 100.00% (3.57) | 91.21 | 97.05 | 97.05 |
| LG14 | 0.21 | 0.43 | 0.14 | 99.81% (5.88) | 97.50% (11.82) | 100.00% (4.43) | 99.53 | 99.90 | 99.90 |
| LG15 | 0.53 | 1.92 | 0.45 | 97.13% (14.10) | 81.63% (13.60) | 99.09% (6.56) | 99.31 | 99.34 | 99.34 |
| LG16 | 0.57 | 0.38 | 0.21 | 99.47% (6.77) | 99.49% (6.17) | 99.71% (6.13) | 98.37 | 99.73 | 99.73 |
| LG17 | 0.27 | 0.52 | 0.21 | 99.68% (8.35) | 98.29% (6.57) | 99.55% (8.35) | 98.02 | 99.10 | 99.10 |
| LG18 | 0.55 | 0.34 | 0.16 | 99.07% (24.28) | 98.43% (14.57) | 100.00% (3.41) | 99.91 | 99.44 | 99.91 |
| LG19 | 0.47 | 0.59 | 0.21 | 98.31% (33.89) | 97.19% (10.21) | 100.00% (4.41) | 97.28 | 96.35 | 97.28 |
| Average | 0.39 | 0.62 | 0.23 | 98.89% | 96.71% | 99.69% | 98.48 | 98.79 | 99.09 |

[b] The coverage is calculated as the ratio of the physical distance between the beginning and the end marker and the total physical distance of each linkage group.

https://doi.org/10.1371/journal.pone.0181728.t004

genetic maps for many plants, including soybean [43], sweet cherry [24], cucumber [44], watermelon [45], red sage [46], and willow [47].

High-throughput sequencing of the SLAF libraries yielded a total of 372.53 M paired-end reads containing 202,349 high-quality SLAFs; the SLAF polymorphism rate was 71.64%. Large-scale SNP markers were developed based on SLAF sequencing data. However, since the presence of some erroneous and missing values in SLAF sequencing data is inevitable, molecular markers must be stringently filtered to avoid false positives [21,48]. Of the 1,762,745 SNPs initially identified, only 77,174 SNPs were considered effective markers for use in the subsequent linkage analysis. These new markers constitute a more effective tool than currently used methods for genetic studies, such as genetic diversity assessment, genetic relationship analysis, and germplasm resource identification [49].

## Construction and importance of grape genetic maps

The development of numerous molecular markers and marker types is a key step for high-density map construction. Several conventional molecular markers, such as RAPDs, AFLPs, SRAPs, and SSRs, were previously widely used to construct grape genetic maps [7–9,11]. Since the construction of the first grape genetic map using RAPD, RFLP, and isozyme markers [6], a number of genetic maps have been developed. However, most current genetic maps contain only a few hundred markers, some of which have no sequence information; LG numbers are also inconsistent in some cases owing to the inefficiency and high genotyping costs of the markers. The saturation, density, and accuracy of currently available genetic maps are thus

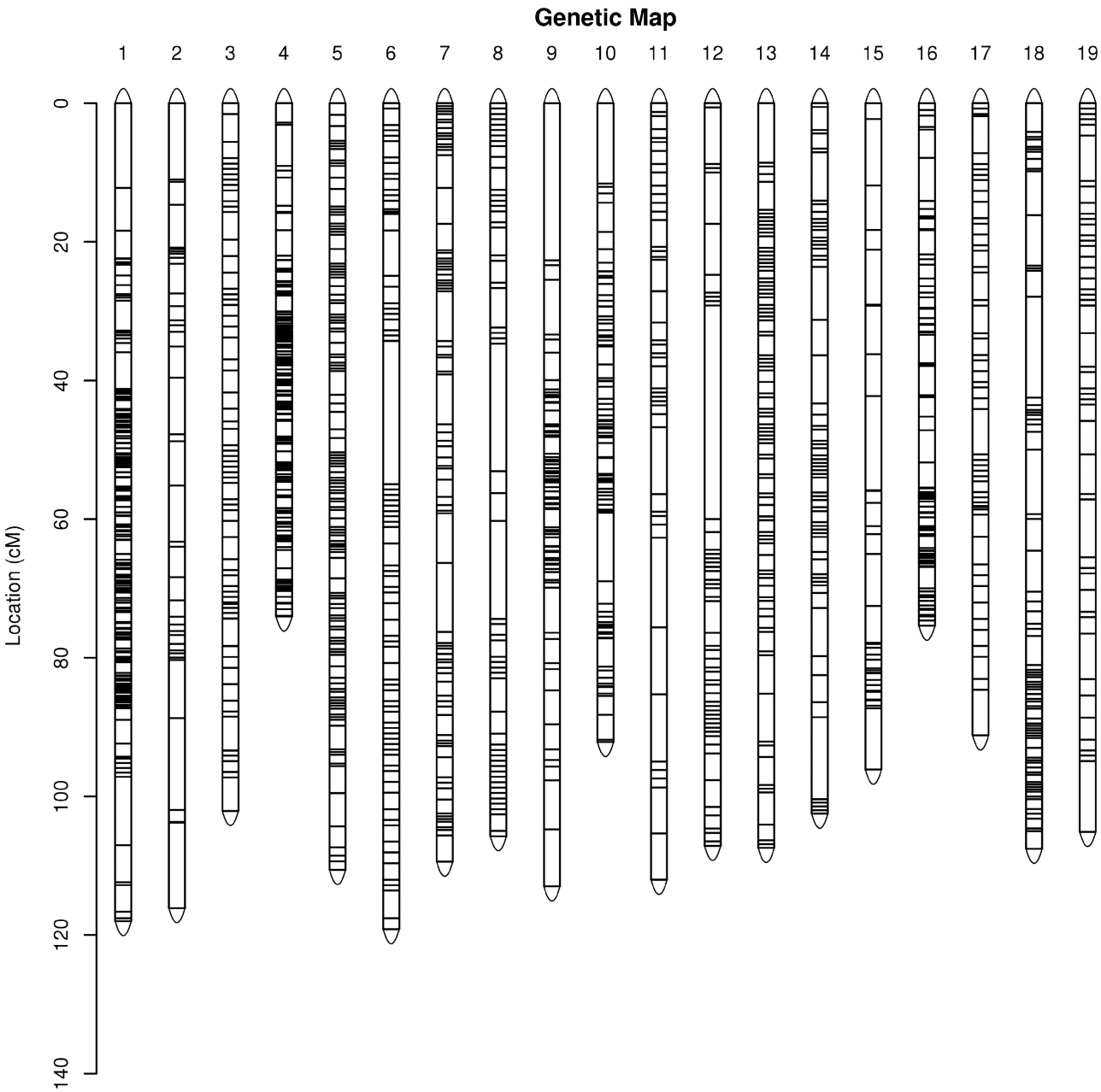


**Fig 3. Genetic map lengths and marker distribution in 19 linkage groups of the male parent.**

https://doi.org/10.1371/journal.pone.0181728.g003

limited [50]. Therefore, it is necessary to rapidly develop large-scale molecular markers for the construction of high-density grape genetic maps.

The development of NGS technology permits the identification of millions of SNP markers across the genome. This technology has been widely used for large-scale genotyping and high-density genetic map construction in several studies. RAD sequencing has been successfully used to construct high-density genetic maps for ryegrass [51], globe artichoke [52], and egg-plant [53]; several maps have been constructed using 2b-RAD sequencing of rice [54], *Brachy-podium distachyon* [55], and bighead carp [56]; and genetic maps for strawberry [57], peanut [58], and lotus [59] have been constructed by ddRAD sequencing. The GBS approach has been

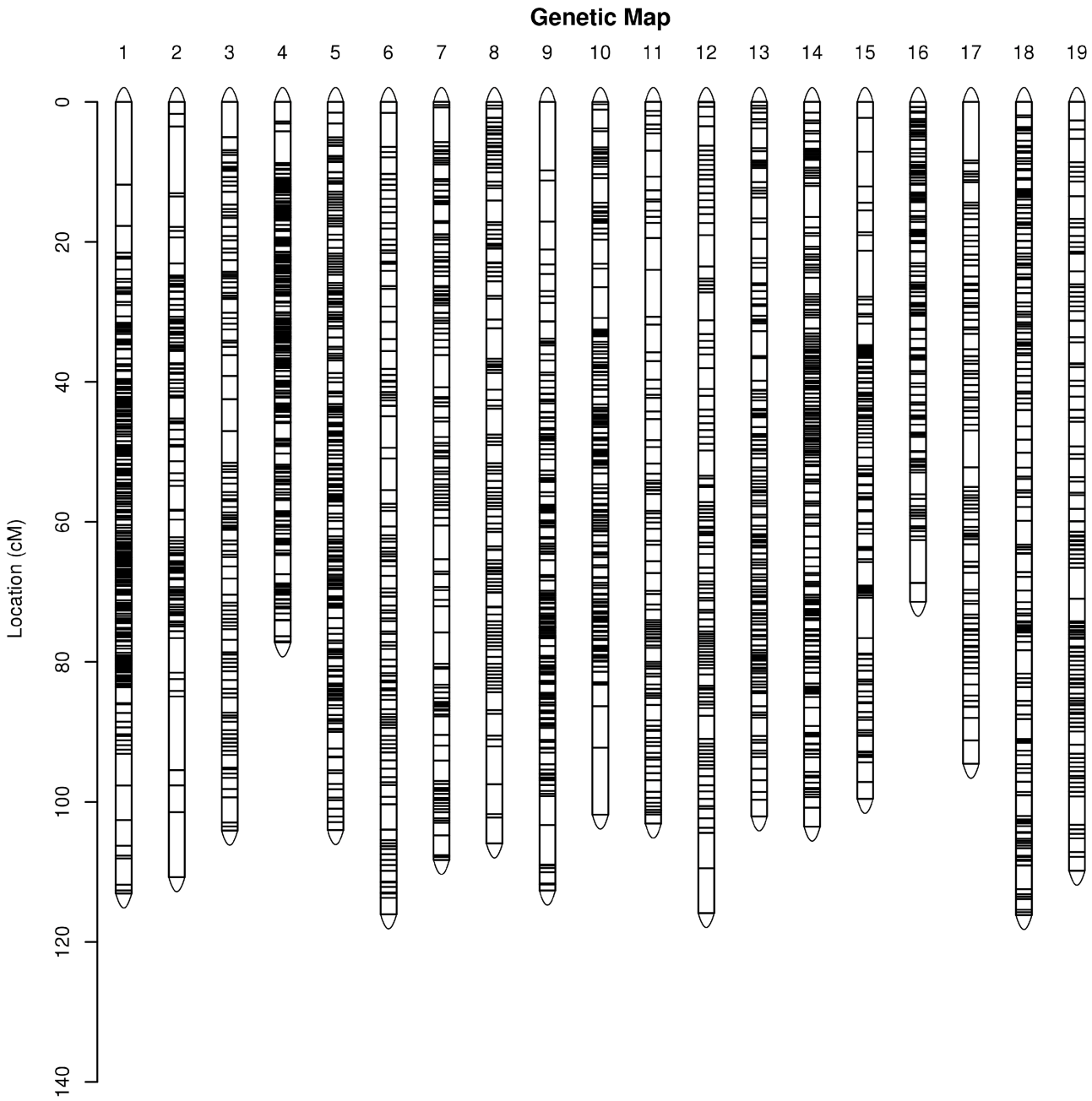


**Fig 4. Genetic lengths and marker distribution in 19 linkage groups of the integrated map.**

https://doi.org/10.1371/journal.pone.0181728.g004

used for the construction of genetic maps of apple [60], barley, and wheat [61]. Recent years have also seen important research progress being made with respect to the construction of high-density genetic maps for grape using NGS technology. Wang et al. [5] constructed a genetic map with 1,646 SNPs and a length of 1,917.13 cM using RAD sequencing. Genetic maps were constructed based on GBS for *V*. *rupestris* 'B38' (1,146 SNPs) and 'Chardonnay' (1,215 SNPs), spanning 1,645 cM and 1,967 cM, respectively [62]. Guo et al. [63] successfully constructed a genetic map with a length of 1929.13 cM containing 7,199 markers using SLAF sequencing. Genetic maps were also obtained from Illumina chips. Using the 18 K Infinium

**Table 5. The Spearman correlation coefficients between the genetic and physical positions of each linkage group on the integrated map.**

| Linkage group ID | Spearman | Linkage group ID | Spearman |
|---|---|---|---|
| LG1 | 0.97 | LG11 | 0.96 |
| LG2 | 0.75 | LG12 | 0.86 |
| LG3 | 0.93 | LG13 | 0.96 |
| LG4 | 0.96 | LG14 | 0.92 |
| LG5 | 0.97 | LG15 | 0.94 |
| LG6 | 0.99 | LG16 | 0.97 |
| LG7 | 0.88 | LG17 | 0.91 |
| LG8 | 0.88 | LG18 | 0.94 |
| LG9 | 0.84 | LG19 | 0.95 |
| LG10 | 0.96 | Average | 0.92 |

https://doi.org/10.1371/journal.pone.0181728.t005

chip, Houel et al. [64] reported genetic maps for 'Picovine' (408 SNPs) and 'Ugni Blanc' (714 SNPs), spanning 606 cM and 1,301 cM, respectively. In the present study, we constructed a high-density genetic map of grape with a total genetic distance of 1,969.95 cM and 10,042 mapped markers. The cover rate of the map length was 99.09%, and the average inter-marker distance was 0.23 cM; the number of mapped markers, average genetic distance, and genome cover rate of the currently reported map present considerable improvements on previously published genetic maps for grape.

Herein, a newly developed HighMap strategy with an iterative process of marker ordering and error genotype correction was applied to construct genetic maps using individual markers; for bin mapping, markers were assigned to bins. A "bin" is a group of markers with a unique segregation pattern and is separated from adjacent bins by a single recombination event. The bin strategy reduces the utilization of genotyping data and recombination information [34]. Therefore, HighMap software may construct a map with higher possible average density depending on the same population size.

Despite these advantages, the constructed map also contained defects such as the presence of several large gaps in sections of the LGs and the weak collinearity of individual LGs. Despite the average distance between adjacent markers on the map being very short (only 0.23 cM), two gaps larger than 10 cM were detected in LG1 and LG2. These large gaps may be due to the absence of marker polymorphism and limited marker detection in these regions [21,65]. Most of the LGs showed good correlation between the genetic and physical positions, but there were also rearrangements in some chromosome regions. Among the 19 LGs, LG2, LG7, LG8, LG9, and LG12 had a lower collinearity compared to other LGs. Imperfect genome assembly, mapping population number, and assembly errors might be common reasons for this inconsistency [66,67]. Moreover, since the male parent 'Beibinghong' is the results of interspecies cross (*V*. *amurensis* × *V*. *vinifera*), some of the regions might originate from *V*. *amurensis* and differ from the reference genome (*V*. *vinifera*). Therefore, the noncollinearity observed in some chromosome regions might indicate the presence of some variations among different grape species that were developed during the course of evolution. We found that many traits in the 130 progenies that bloomed and fruited in 2016 were segregated. In the future, we intend to increase the mapping population size in order to improve map saturation. This improved map will lay the foundation for QTL mapping and identification of candidate genes related to major economic and agronomic traits.

SLAF-seq is a promising rapid and cost-effective strategy for the construction of high-density genetic maps to facilitate the incorporation of desirable traits in cultivated grapes. In this study, 202,349 high-quality SLAFs were developed using the SLAF-seq method. Large-scale

SNP markers were developed and used for the construction of a high-density genetic map for grape. A total of 10,042 mapped markers were distributed in 19 LGs. The genetic map spanned 1,969.95 cM with an average inter-marker distance of 0.23 cM. Furthermore, this map will serve as a valuable tool for grape breeders for genetic or QTL mapping or association mapping of important agronomic traits, map-based gene cloning, comparative mapping, and marker-assisted breeding.

## Supporting information

**S1 Fig. Correlation of genetic and physical positions.** The x-axis represents the genetic distance of each linkage group (LG); the y-axis represents the physical position of each LG.
(TIF)

**S1 File. Haplotype map of the genetic map.** Each two columns represent the genotype of an individual. The first column of each individual represents 'Beibinghong' (the male parent); the second column of each individual represents 'Chardonnay' (the female parent). Rows correspond to genetic markers. Green indicates the first allele from the parent, blue refers to the second allele from the parent, and gray denotes missing data.
(ZIP)

**S2 File. Heat map of the genetic map.** Each cell represents the recombination rate of two markers. Yellow and purple indicate lower and higher recombination rates, respectively. Gray denotes missing data.
(ZIP)

**S3 File. Marker genotypes used for mapping.** "–" represents missing data.
(XLSX)

## Author Contributions

**Formal analysis:** Jiahui Wang, Kai Su.

**Funding acquisition:** Xiuwu Guo.

**Investigation:** Huiyang Xing, Yuhui Zhao, Zhendong Liu, Kun Li.

**Project administration:** Yinshan Guo.

**Resources:** Xiuwu Guo.

**Supervision:** Xiuwu Guo.

**Writing – original draft:** Jiahui Wang.

**Writing – review & editing:** Jiahui Wang, Kai Su, Yinshan Guo.

## References

1. Bertelli A A, Das DK. Grapes, wines, resveratrol, and heart health. J Cardiovasc Pharmacol. 2009; 54 (6): 468–476. https://doi.org/10.1097/FJC.0b013e3181bfaff3 PMID: 19770673
2. Dohadwala MM, Vita JA. Grapes and cardiovascular disease. J Nutr. 2009; 139 (9): 1788S–1793S. https://doi.org/10.3945/jn.109.107474 PMID: 19625699
3. Pezzuto JM, Venkatasubramanian V, Hamad M, Morris KR. Unraveling the relationship between grapes and health. J Nutr. 2009; 139(9): 1783S–1787S. https://doi.org/10.3945/jn.109.107458 PMID: 19625701
4. Wu CD. Grape products and oral health. J Nutr. 2009; 139(9): 1818S–1823S. https://doi.org/10.3945/jn.109.107854 PMID: 19640974

5. Wang N, Fang LC, Xin HP, Wang LJ, Li SH. Construction of a high-density genetic map for grape using next generation restriction-site associated DNA sequencing. BMC Plant Biol. 2012; 12: 148. https://doi.org/10.1186/1471-2229-12-148 PMID: 22908993
6. Lodhi MA, Daly MJ, Ye GN, Weeden NF, Reisch BI. A molecular marker based linkage map of *Vitis*. Genome. 1995; 38(4): 786–794. PMID: 7672609
7. Dalbó MA, Ye GN, Weeden NF, Steinkellner H, Sefc K M, Reisch BI. A gene controlling sex in grapevines placed on a molecular marker-based genetic map. Genome. 2000; 43(2): 333–340. PMID: 10791822
8. Doucleff M, Jin Y, Gao F, Riaz S, Krivanek AF, Walker MA. A genetic linkage map of grape, utilizing *Vitis rupestris* and *Vitis arizonica*. Theor Appl Genet. 2004; 109 (6): 1178–1187. https://doi.org/10.1007/s00122-004-1728-3 PMID: 15292989
9. Liu ZD, Guo XW, Guo YS, Lin H, Zhang PX, Zhao YH, et al. SSR and SRAP markers based linkage map of *Vitis Amurensis* rupr. Pak J Bot. 2013; 45(1): 191–195.
10. Riaz S, Dangl GS, Edwards KJ, Meredith CP. A microsatellite marker based framework linkage map of *Vitis vinifera* L. Theor Appl Genet. 2004; 108(5): 864–872. https://doi.org/10.1007/s00122-003-1488-5 PMID: 14605808
11. Moreira FM, Madini A, Marino R, Zulini L, Stefanini M, Velasco R, et al. Genetic linkage maps of two interspecific grape crosses (*Vitis* spp.) used to localize quantitative trait loci for downy mildew resistance. Tree Genet Genomes. 2011; 7(1): 153–167. https://doi.org/10.1007/s11295-010-0322-x
12. Pap D, Riaz S, Dry IB, Jermakow A, Tenscher AC, Cantu D, et al. Identification of two novel powdery mildew resistance loci, Ren6 and Ren7, from the wild Chinese grape species *Vitis piasezkii*. BMC Plant Biol. 2016; 16:170. https://doi.org/10.1186/s12870-016-0855-8 PMID: 27473850
13. Jaillon O, Aury JM, Noel B, Policriti A, Clepet C, Casagrande A, et al. The grapevine genome sequence suggests ancestral hexaploidization in major angiosperm phyla. Nature. 2007; 449(7161): 463–467. https://doi.org/10.1038/nature06148 PMID: 17721507
14. Varshney RK, Nayak SN, May GD, Jackson SA. Next-generation sequencing technologies and their implications for crop genetics and breeding. Trends Biotech. 2009; 27(9): 522–530. https://doi.org/10.1016/j.tibtech.2009.05.006 PMID: 19679362
15. Liu J, Huang S, Sun M, Liu S, Liu Y, Wang W, et al. An improved allele-specific PCR primer design method for SNP marker analysis and its application. Plant Methods. 2012; 8(1): 34. https://doi.org/10.1186/1746-4811-8-34 PMID: 22920499
16. Ward JA, Bhangoo J, Fernández-Fernández F, Moore P, Swanson JD, Viola R, et al. Saturated linkage map construction in *Rubus idaeus* using genotyping by sequencing and genome-independent imputation. BMC Genomics. 2013; 14(1): 2. https://doi.org/10.1186/1471-2164-14-2 PMID: 23324311
17. Baird NA, Etter PD, Atwood TS, Currey MC, Shiver AL, Lewis ZA, et al. Rapid SNP discovery and genetic mapping using sequenced RAD markers. PLoS One. 2008; 3(10): e3376. https://doi.org/10.1371/journal.pone.0003376 PMID: 18852878
18. Wang S, Meyer E, Mckay JK, Matz MV. 2b-RAD: a simple and flexible method for genome-wide genotyping. Nat Methods. 2012; 9(8): 808–810. https://doi.org/10.1038/nmeth.2023 PMID: 22609625
19. Dacosta JM, Sorenson MD. Amplification biases and consistent recovery of loci in a double-digest RAD-seq protocol. PloS One. 2014; 9(9): e106713. https://doi.org/10.1371/journal.pone.0106713 PMID: 25188270
20. Elshire RJ, Glaubitz JC, Sun Q, Poland J A, Kawamoto K, Buckler ES, et al. A robust, simple Genotyping-by-Sequencing (GBS) approach for high diversity species. PLoS One. 2011; 6 (5): e19379. https://doi.org/10.1371/journal.pone.0019379 PMID: 21573248
21. Sun X, Liu D, Zhang X, Li W, Liu H, Hong W, et al. SLAF-seq: an efficient method of large-scale *De novo* SNP discovery and genotyping using high-throughput sequencing. PloS One. 2013; 8(3): e58700. https://doi.org/10.1371/journal.pone.0058700 PMID: 23527008
22. Zhang Y, Wang L, Xin H, Li D, Ma C, Ding X, et al. Construction of a high-density genetic map for sesame based on large scale marker development by specific length amplified fragment (SLAF) sequencing. BMC Plant Biol. 2013; 13: 141. https://doi.org/10.1186/1471-2229-13-141 PMID: 24060091
23. Jiang B, Liu W. Xie D, Peng Q, He X, Lin Y, et al. High-density genetic map construction and gene mapping of pericarp color in wax gourd using specific-locus amplified fragment (SLAF) sequencing. BMC Genomics. 2015; 16: 1035. https://doi.org/10.1186/s12864-015-2220-y PMID: 26647294
24. Wang J, Zhang K, Zhang X, Yan G, Zhou Y, Feng L, et al. Construction of commercial sweet cherry linkage maps and QTL analysis for trunk diameter. PLoS One. 2015; 10(10): e0141261. https://doi.org/10.1371/journal.pone.0141261 PMID: 26516760

25. Bai ZY, Han XK, Liu XJ, Li QQ, Li JL. Construction of a high-density genetic map and QTL mapping for pearl quality-related traits in *Hyriopsis cumingii*. Sci Rep. 2016; 6: 32608. https://doi.org/10.1038/srep32608 PMID: 27587236

26. Yu Y, Zhang X, Yuan J, Li F, Chen X, Zhao Y, et al. Genome survey and high-density genetic map construction provide genomic and genetic resources for the Pacific White Shrimp *Litopenaeus vannamei*. Sci Rep. 2015; 5: 15612. https://doi.org/10.1038/srep15612 PMID: 26503227

27. Song R, Lu W, Shen Y, Jin R, Li X, Guo Z, et al. A new ice-red wine grape variety—Beibinghong. Sino-Overseas Grapevine and Wine. 2008; 4: 19–22.

28. Hanania U, Velcheva M, Sahar N, Perl A. An improved method for isolating high-quality DNA from *Vitis vinifera* nuclei. Plant Mol Biol Rptr. 2004; 22: 173–177. https://doi.org/10.1007/BF02772724

29. Zhang J, Zhang Q, Cheng T, Yang W, Pan H, Zhong J, et al. High-density genetic map construction and identification of a locus controlling weeping trait in an ornamental woody plant (*Prunus mume* Sieb. et Zucc). DNA Res. 2015; 22(3): 183–191. https://doi.org/10.1093/dnares/dsv003 PMID: 25776277

30. Jaillon O, Aury JM, Noel B, Policriti A, Clepet C, Casagrande A, et al. The grapevine genome sequence suggests ancestral hexaploidization in major angiosperm phyla. Nature. 2007; 449(7161): 463–467. https://doi.org/10.1038/nature06148 PMID: 17721507

31. Li H, Durbin R. Fast and accurate short read alignment with Burrows-Wheeler transform. Bioinformatics. 2009; 25(14): 1754–1760. https://doi.org/10.1093/bioinformatics/btp324 PMID: 19451168

32. DePristo MA, Banks E, Poplin R., Garimella KV, Maguire JR, Hartl C, et al. A framework for variation discovery and genotyping using next-generation DNA sequencing data. Nat Genet. 2011; 43: 491–498. https://doi.org/10.1038/ng.806 PMID: 21478889

33. Li H, Handsaker B, Wysoker A, Fennell T, Ruan J, Homer N, et al. The sequence Alignment/Map format and SAMtools. Bioinformatics. 2009; 25: 2078–2079. https://doi.org/10.1093/bioinformatics/btp352 PMID: 19505943

34. Liu D, Ma C, Hong W, Huang L, Liu M, Liu H, et al. Construction and analysis of high-density linkage map using high-throughput sequencing data. PloS One. 2014; 9(6): e98855. https://doi.org/10.1371/journal.pone.0098855 PMID: 24905985

35. Jansen J, de Jong A, van Ooijen J. Constructing dense genetic linkage maps. Theor Appl Genet. 2001; 102: 1113–1122. https://doi.org/10.1007/s001220000489

36. van Ooijen J. Multipoint maximum likelihood mapping in a full-sib family of an outbreeding species. Genet Res. 2011; 93(5): 343–349. https://doi.org/10.1017/S0016672311000279 PMID: 21878144

37. van Os H, Stam P, Visser RG, van Eck H J. SMOOTH: a statistical method for successful removal of genotyping errors from high-density genetic linkage data. Theor Appl Genet. 2005; 112(1): 187–194. https://doi.org/10.1007/s00122-005-0124-y PMID: 16258753

38. Huang X, Zhao Y, Wei X, Li C, Wang A, Zhao Q, et al. Genome-wide association study of flowering time and grain yield traits in a worldwide collection of rice germplasm. Nat Genet. 2011; 44(1): 32–39. https://doi.org/10.1038/ng.1018 PMID: 22138690

39. Kosambi DD. The estimation of map distances from recombination values. Ann Hum Genet. 1943; 12 (1): 172–175. https://doi.org/10.1111/j.1469-1809.1943.tb02321.x

40. Liu L, Qu C, Wittkop B, Yi B, Xiao Y, He Y, et al. A high-density SNP map for accurate mapping of seed fibre QTL in *Brassica napus* L. PLoS One. 2013; 8:e83052. https://doi.org/10.1371/journal.pone.0083052 PMID: 24386142

41. Sim S-C, Durstewitz G, Plieske J, Wieseke R, Ganal MW, van Deynze A, et al. Development of a large SNP genotyping array and generation of high-density genetic maps in tomato. PLoS One. 2012; 7(7): e40563. https://doi.org/10.1371/journal.pone.0040563 PMID: 22802968

42. West MAL, van Leeuwen H, Kozik A, Kliebenstein DJ, Doerge RW, St Clair DA, et al. High-density haplotyping with microarray-based expression and single feature polymorphism markers in Arabidopsis. Genome Res. 2006; 16: 787–795. https://doi.org/10.1101/gr.5011206 PMID: 16702412

43. Qi ZM, Huang L, Zhu RS, Xin DW, Liu CY, Han X, et al. A high-density genetic map for soybean based on specific length amplified fragment sequencing. PloS One. 2014; 9 (8): e104871. https://doi.org/10.1371/journal.pone.0104871 PMID: 25118194

44. Xu WW, Xu RX, Zhu BY, Yu T, Qu WQ, Lu L., et al. A high-density genetic map of cucumber derived from specific length amplified fragment sequencing (SLAF-seq). Front Plant Sci. 2015; 5: 768. https://doi.org/10.3389/fpls.2014.00768 PMID: 25610449

45. Shang JL, Li N, Li NN, Xu YY, Ma SW, Wang JM. Construction of a high-density genetic map for watermelon (*Citrullus lanatus* L.) based on large-scale SNP discovery by specific length amplified fragment sequencing (SLAF-seq). Scientia Hort. 2016; 203: 38–46. https://doi.org/10.1016/j.scienta.2016.03.007

46. Liu T, Guo LL, Pan YL, Zhao Q, Wang JH, Song ZQ. Construction of the first high-density genetic linkage map of *Salvia miltiorrhiza* using specific length amplified fragment (SLAF) sequencing. Sci Rep. 2016; 6: 24070. https://doi.org/10.1038/srep24070 PMID: 27040179

47. Zhang J, Yuan HW, Li M, Li YJ, Wang Y, Ma XJ, et al. A high-density genetic map of tetraploid *Salix matsudana* using specific length amplified fragment sequencing (SLAF-seq). Plos One. 2016; 11(6): e0157777. https://doi.org/10.1371/journal.pone.0157777 PMID: 27327501

48. Zhang YX, Wang LH, Xin HG, Li DH, Ma CX, Ding X, et al. Construction of a high-density genetic map for sesame based on large scale marker development by specific length amplified fragment (SLAF) sequencing. BMC Plant Biol. 2013; 13: 141. https://doi.org/10.1186/1471-2229-13-141 PMID: 24060091

49. Zhang C, Wang Y, Fu J, Dong L, Gao S, Du D. Transcriptomic analysis of cut tree peony with glucose supply using the RNA-Seq technique. Plant Cell Rep. 2014; 33(1): 111–129. https://doi.org/10.1007/s00299-013-1516-0 PMID: 24132406

50. Kakioka R, Kokita T, Kumada H, Watanabe K, Okuda N. A RAD-based linkage map and comparative genomics in the gudgeons (genus Gnathopogon, Cyprinidae). BMC Genomics. 2013; 14: 32. https://doi.org/10.1186/1471-2164-14-32 PMID: 23324215

51. Pfender WF, Saha MC, Johnson EA, Slabaugh MB. Mapping with RAD (restriction-site associated DNA) markers to rapidly identify QTL for stem rust resistance in Lolium perenne. Theor Appl Genet. 2011; 122(8): 1467–1480. https://doi.org/10.1007/s00122-011-1546-3 PMID: 21344184

52. Scaglione D, Acquadro A, Portis E, Tirone M, Knapp SJ, Lanteri S. RAD tag sequencing as a source of SNP markers in *Cynara cardunculus* L. BMC Genomics. 2012; 13:3. https://doi.org/10.1186/1471-2164-13-3 PMID: 22214349

53. Barchi L, Lanteri S, Portis E, Acquadro A, Vale G, Toppino L, et al. Identification of SNP and SSR markers in eggplant using RAD tag sequencing. BMC Genomics. 2011; 12: 304. https://doi.org/10.1186/1471-2164-12-304 PMID: 21663628

54. Guo Y, Yuan H, Fang D, Song L, Liu Y, Liu Y, et al. An improved 2b-RAD approach (I2b-RAD) offering genotyping tested by a rice (Oryza sativa L.) F2 population. BMC Genomics. 2014; 15: 956. https://doi.org/10.1186/1471-2164-15-956 PMID: 25373334

55. Des Marais DL, Razzaque S, Hernandez KM, Garvin DF, Juenger TE. Quantitative trait loci associated with natural diversity in water-use efficiency and response to soil drying in Brachypodium distachyon. Plant Sci. 2016; 251: 2–11. https://doi.org/10.1016/j.plantsci.2016.03.010 PMID: 27593458

56. Fu B, Liu H, Yu X, Tong J. A high-density genetic map and growth related qtl mapping in bighead carp (*Hypophthalmichthys nobilis*). Sci Rep. 2016; 6: 28679. https://doi.org/10.1038/srep28679 PMID: 27345016

57. Davik J, Sargent DJ, Brurberg MB, Lien S, Kent M, Alsheikh M. A ddRAD based linkage map of the cultivated strawberry, *Fragaria xananassa*. PLoS One. 2015; 10(9): e0137746. https://doi.org/10.1371/journal.pone.0137746 PMID: 26398886

58. Zhou X, Xia Y, Ren X, Chen Y, Huang L, Huang S, et al. Construction of a SNP-based genetic linkage map in cultivated peanut based on large scale marker development using next-generation double-digest restriction-site-associated DNA sequencing (ddRADseq). BMC Genomics. 2014; 15: 351. https://doi.org/10.1186/1471-2164-15-351 PMID: 24885639

59. Liu Z, Zhu H, Liu Y, Kuang J, Zhou K, Liang F, et al. Construction of a high-density, high-quality genetic map of cultivated lotus (*Nelumbo nucifera*) using next-generation sequencing. BMC Genomics. 2016; 17: 466. https://doi.org/10.1186/s12864-016-2781-4 PMID: 27317430

60. Kyle MG, Patrick B, Thomas FC, Scott C, Fabrizio C, Carlos B, et al. Fast and cost-effective genetic mapping in apple using next-generation sequencing. Genes Genom Gene. 2014; 4(9): 1681–1687. https://doi.org/10.1534/g3.114.011023 PMID: 25031181

61. Poland JA, Brown PJ, Sorrells ME, Jannink J-L. Development of high-density genetic maps for barley and wheat using a novel two-enzyme genotyping-by-sequencing approach. PLoS One. 2012; 7(2): e32253. https://doi.org/10.1371/journal.pone.0032253 PMID: 22389690

62. Barba P, Cadle-Davidson L, Harriman J, Glaubitz JC, Brooks S, Hyma K, et al. Grapevine powdery mildew resistance and susceptibility loci identified on a high-resolution SNP map. Theor Appl Genet. 2014; 127: 73–84. https://doi.org/10.1007/s00122-013-2202-x PMID: 24072208

63. Guo Y S, Shi GL, Liu ZD, Zhao YH, Yang XX, Zhu JC, et al. Using specific length amplified fragment sequencing to construct the high-density genetic map for *Vitis* (*Vitis vinifera* L.× *Vitis amurensis* Rupr.). Front Plant Sci. 2015; 6: 393. https://doi.org/10.3389/fpls.2015.00393 PMID: 26089826

64. Houel C, Chatbanyong R, Doligez A, Rienth M, Foria S, Luchaire N, et al. Identification of stable QTLs for vegetative and reproductive traits in the microvine (*Vitis vinifera* L.) using the 18 K Infinium chip. BMC Plant Biol. 2015; 15: 205. https://doi.org/10.1186/s12870-015-0588-0 PMID: 26283631

65. Wang W, Huang S, Liu Y, Fang Z, Yang L, Hua W, et al. Construction and analysis of a highdensity genetic linkage map in cabbage (*Brassica oleracea* L. var. capitata). BMC Genomics. 2012; 13: 523. https://doi.org/10.1186/1471-2164-13-523 PMID: 23033896

66. Lin Y, Li J, Shen H, Zhang L, Papasian CJ, Deng HW. Comparative studies of *de novo* assembly tools for next-generation sequencing technologies. Bioinformatics. 2011; 27(15): 2031–2037. https://doi.org/10.1093/bioinformatics/btr319 PMID: 21636596

67. Zhang Q, Liu C, Liu Y, van Buren R, Yao X, Zhong C, et al. High-density interspecific genetic maps of kiwifruit and the identification of sex-specific markers. DNA Res. 2015; 22: 367–375. https://doi.org/10.1093/dnares/dsv019 PMID: 26370666